Journal of Alloys and Compounds 770 (2019) 166–174

Contents lists available at ScienceDirect

Journal of Alloys and Compounds

journal homepage: http://www.elsevier.com/locate/jalcom

Effective solution treatment can result in improved creep performance of superalloys

Chonglin Jia*, Fenglin Zhang, Kang Wei, Shaomin Lv

Science and Technology on Advanced High Temperature Structural Materials Laboratory, Beijing Institute of Aeronautical Materials, Beijing, 100095, China

ARTICLE INFO

Article history:
Received 11 March 2018
Received in revised form
2 August 2018
Accepted 9 August 2018
Available online 11 August 2018

Keywords:
Superalloy
Solution treatment
Creep performance
Deformation mechanism
Fracture characteristics
Dislocations

ABSTRACT

Herein, we demonstrate the creep performance of a turbine disk superalloy – FGH100L – at 705 °C and 897 MPa. The effect of solution treatment and cooling rate on the microstructure, fracture and creep performance is presented in detail. The microstructure and fracture are characterized by optical microscopy (OM), transmission electron microscopy (TEM) and scanning electron microscopy (SEM). The results reveal that instead of air cooling (AC), after solution treatment (ST), the combination of slow and fast cooling improves the creep performance of the alloy at 705 °C and 897 MPa. Both during AC and the combination of slow and fast cooling, followed by ST, the creep process is dominated by the accumulation of dislocations and stacking faults, cutting through the γ′ phase. The microstructural evolution is the main cause of creep acceleration, which mainly manifests as coarsening and morphology change of the γ′ phase. Our proposed heat treatment scheme generates the serrated grain boundaries, which play a vital role in improving the creep performance. In the case of AC, the creep pores sprout and develop into wedge-shaped cracks at the trigeminal intersection of the grain boundary, while the combination of slow and fast cooling results in opening-mode cracks at the grain boundary and carbide interface. Both creep ruptures, under two different heat treatment processes, are intergranular fractures.

1. Introduction

The nickel-based superalloy is an important material for manufacturing the critical hot section turbine disk components of the aero engine [1,2]. The increased thrust-to-weight ratio in advanced aircraft requires higher inlet temperature to the turbine [3], which demands excellent thermal and mechanical properties of the superalloy [4]. Also, the high temperature creep performance is a significant parameter to assess the temperature-dependent mechanical properties of the superalloy. In addition, the creep performance of nickel-based superalloys depends largely on the γ′ phase and grain structure [5–11]. For example, Sugui et al. studied the interaction between the γ′ phase and dislocations of the FGH95 alloy at various temperatures (630–650 °C) and applied stress levels (984–1034 MPa) and discussed the creep mechanism [12]. Goff et al. investigated the creep performance of the Udimet 720 alloy with coarse and fine grain structure and established the creep damage model [13]. Probstle et al. explored the creep behavior of the Allvac 718Plus alloy and the effect of the γ′-denuded zone at 650 °C/800 MPa, after 670 °C thermal exposure [14].

Furthermore, the heat treatment (HT) process, consisting of a solution and aging treatment, is performed to achieve the optimal microstructure and mechanical properties of the superalloy [15,16]. A couple of studies have revealed that the cooling rate, after solution treatment (ST), affects the size and morphology of the γ′ precipitates and the rapid cooling results in finer intragranular γ′ precipitates [17,18]. However, the rapid cooling after ST, such as by quenching in water, increases the propensity for quench cracking during disk forging [19], which implies that the cooling rate needs to be optimized to attain the desired microstructure, without introducing cracks. The FGH100L is a γ′ phase precipitation strengthened nickel-based superalloy with a γ′ phase volume fraction of about 55%, which can be used to manufacture the turbine disk at the service temperature of 750 °C or above it. The HT of this alloy includes ST and two-step aging treatment (AT). However, the effect of ST on the microstructure and creep properties of the alloy has not been examined yet.

In this paper, we report the influence of ST on the microstructure and creep behavior of the alloy. In this study, the spray-formed superalloy FGH100L disk forging is achieved using two kinds of

* Corresponding author.
E-mail address: biamjcl@163.com (C. Jia).

https://doi.org/10.1016/j.jallcom.2018.08.089
0925-8388/

ST systems, followed by two-step air cooling (AC). The creep behavior and microstructural evolution of FGH100L alloys, treated through different solution processes, were also observed. The findings of this study provide a theoretical basis to optimize the HT process and develop the alloy with the desired set of properties.

2. Materials and processes

The FGH100L superalloy billets were prepared by the spray-forming deposition process. The spray-formed billets had a diameter of 190 mm and a height of 270 mm. The chemical composition (mass fraction) of the billet was C (0.032), Cr (12.50), W (4.30), Mo (2.80), Co (21.34), Al (3.52), Ti (3.34), Nb (1.35), Ta (1.60), and Ni (balance). At 1145 °C and 150 MPa, the deposited billet was subjected to hot isostatic pressing and densification treatment. Then, using the line cutting method, the billet was cut in the longitudinal direction into four sections of about φ190 mm × 65 mm. One of the sections, adopted with about 35% of the amount of deformation, was isothermally forged to produce pancake-shaped forgings with a diameter of 236 mm and a height of 40 mm. The bars for mechanical characterization were cut off from the disc forgings with a wire cutting machine. Two solution HT schemes were used for the bars, referred to henceforth as Process-A and Process-B. In Process-A, the test bars were heated to 1140 °C, held at such temperature for 1 h and then subjected to AC, i.e., cooled down to room temperature at the cooling rate of 30 °C/min. In Process-B, the test bars were heated to 1140 °C, insulated for one hour and then slowly cooled down to room temperature at the cooling rate of 5 °C/min. These bars were heated again to 1110 °C, insulated for 1 h and rapidly cooled down to room temperature at the cooling rate of 110 °C/min. After the ST, both kinds of test bars were subjected to a two-step aging process at 850 °C for 4 h, and 770 °C for 8 h, followed by AC.

According to China's national standard Metallic Materials—Creep and Stress-Rupture Test in Tension (GB2039), the test bars were machined to prepare creep specimens, with a gauge diameter of 5 mm and gauge length of 25 mm. The creep test for the two specimens was carried out at 705 °C and under 897 MPa stress.

The microstructure, before the creep test, was observed with a Leica DMR positive field metallographic microscope (Leica Wetzlar, Heidelberg, Germany). The samples were mechanically polished and etched using 5 g $FeCl_3$ and 100 mL HCl etchant. The transmission electron microscopy (TEM) analysis of the fractured samples was performed on a FEI Tecnai G2 F20 field emission gun transmission electron microscope (FEI Company, Hillsboro, OR, USA), operating at 200 kV. The TEM samples were cut off from the broken creep specimens, 1 mm above the fracture, and used to examine the morphology of the γ′ strengthening phase and dislocation structure. The TEM foil specimens were prepared by a conventional method, consisting of mechanical grinding and polishing to lamellas of 3-mm diameter, followed by twin-jet electropolishing with a solution of 10% perchloric acid and 90% ethanol at −30 °C. The field emission scanning electron microscopy (FESEM) samples were prepared by electrolytic polishing, with a solution of 20% H_2SO_4 and 80% CH_3OH, for 30–40s and electrolytic etching, with a solution of 9 g CrO_3, 90 mL H_3PO_4 and 30 mL C_2H_5OH, at 5 V for 3–5 s, after mechanical polishing. The γ'/γ microstructure and creep morphology were observed on a FEI Nova NanoSEM 450 field emission scanning electron microscope (FEI company), equipped with an energy spectrum analyzer.

3. Results and analysis

3.1. The original microstructure of creep specimens

3.1.1. The original grain microstructure

The images displayed in Fig. 1 show the grain morphology of the alloy under two processes, which reveal that they are basically equiaxed grains with similar grain size. However, the grain boundaries (GBs) are very different under the two HT processes. Process-A resulted in smooth and straight GBs (Fig. 1a), whereas Process-B resulted in highly serrated GBs (Fig. 1b and inset). The serrated GBs were developed after HT by slow cooling (SC) and fast cooling (FC). Therefore, the curved saw-tooth GBs were obtained by Process-B.

3.1.2. Characteristics of γ′ precipitates after ST

In order to further understand the effect of different ST processes on intra- and inter-granular precipitates and GBs, the γ/γ′ microstructure was observed using the backscattered electron mode of FESEM. The γ′ precipitate microstructure, which forms in two kinds of ST is shown in Fig. 2. The images in Fig. 2 reveal that a small number of larger primary γ′ precipitates are distributed in the GBs of the alloy and a large number of smaller γ′ precipitates are distributed inside the grains after different HT processes.

The overall size of the γ′ particles within the grain, after treatment by Process-A, was relatively large and the majority of the particles were in the size range from 0.3 to 0.6 μm. However, following the treatment by Process-B, the intragranular γ′ particle size distribution ranged from 50 to 200 nm, with an average particle size of about 150 nm. Thus, it can be concluded that Process-B resulted in γ′ precipitates refinement.

The reason for the above results is that during the SC process, the γ′ precipitates grow up completely and result in larger γ′ particles with uneven distribution at the GBs. Moreover, the presence of coarse γ′ particles prevents the GB migration, whereas the GB between the γ′ particles moves towards the inner grain and

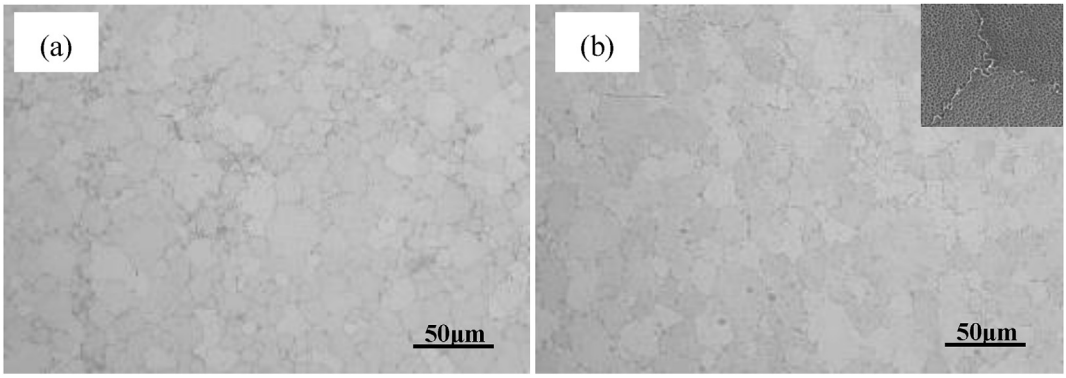

Fig. 1. The grain morphology of FGH100L forged disks after heat treatment: (a) Process-A and (b) Process-B.